

PSFC/JA-10-13

**Divertor heat flux footprints in EDA
H-mode discharges on Alcator C-Mod**

LaBombard, B., Terry, J.L., Hughes, J.W., Brunner, D., Payne, J.,
Reinke, M.L., Lin, Y., Wukitch, S.

June 2010

**Plasma Science and Fusion Center
Massachusetts Institute of Technology
Cambridge MA 02139 USA**

This work was supported by the U.S. Department of Energy, Grant No. DE-FC02-99ER54512. Reproduction, translation, publication, use and disposal, in whole or in part, by or for the United States government is permitted.

Divertor heat flux footprints in EDA H-mode discharges on Alcator C-Mod

B. LaBombard*, J.L. Terry, J.W. Hughes, D. Brunner,

J. Payne, M.L. Reinke, Y. Lin, S. Wukitch

Plasma Science and Fusion Center

Massachusetts Institute of Technology, Cambridge, MA 02139, USA

The physics that sets the width of the power exhaust channel in a tokamak scrape-off layer and its scaling with engineering parameters is of fundamental importance for reactor design, yet it remains to be understood. An extensive array of divertor heat flux diagnostics was recently commissioned in Alcator C-Mod with the aim of improving our understanding. Initial results are reported from EDA H-mode discharges in which plasma current, input power, toroidal field and magnetic topology were varied. The integral width of the outer divertor heat flux footprint is found to lie in the range of 3 to 5 mm mapped to the midplane. Widths are insensitive to single versus double-null topology and the magnitude of toroidal field. Pedestal physics appears to largely determine these widths; a dependence of width on plasma thermal energy is noted, yielding a reduction in width as plasma current is increased for the best EDA H-modes.

PACS: 52.25.Fi Transport Properties, 52.40.Hf Plasma-material interactions; boundary layer effects, 52.55.Rk Power exhaust; divertors, 52.70.Kz Optical measurements

1. Introduction

Physics-based transport models that can accurately simulate heat-flux power widths in the tokamak boundary plasma are lacking at the present time. Yet this quantity is of fundamental importance for ITER and most critically for DEMO. Recognizing the importance of this science area, C-Mod, DIII-D and NSTX are performing coordinated experiments in 2010, aimed at characterizing divertor heat flux ‘footprints’ and their connections to conditions in the boundary and core plasmas. Until recently, C-Mod was not equipped to measure divertor heat fluxes. In support of the experimental program, an extensive array of divertor diagnostics was installed in 2009, including IR thermography, embedded calorimeters, tile thermocouples and surface thermocouples. This paper briefly introduces the new diagnostic set and reports initial observations of heat flux footprints and their dependences in EDA H-mode discharges.

2. New divertor heat flux diagnostics

An array of embedded heat-flux sensor probes (tile thermocouples, calorimeters, surface thermocouples) combined with a new IR camera (ElectroPhysics Titanium 550M [This camera, now sold as the FLIR SC7000, was supplied through C-Mod’s collaboration with LANL, DoE Award DE-AC52-06NA25396.]) was installed during C-Mod’s 2009 maintenance period (see Fig.1). Instrumented tiles on the outer divertor consist of two vertical columns, tilted in the toroidal direction by ~ 2 degrees and ‘ramped up’ by 2 mm relative to standard tiles. This ensures that the instrumented tiles will not be shadowed by misalignments. It also increases the thermal load to the ramped tiles, improving signal-to-noise for sensor-based diagnostics.

The IR camera views the ramped tiles by looking both down and in the toroidal direction from a periscope [1], which is located in a vertical port ~ 90 degrees away. An example image is shown in Fig. 1. IR thermography is challenging in C-Mod with its shiny,

low emissivity tile surfaces and oblique observations angles [2] – an environment that is similar to ITER. Additional complications include low-Z surface films (boron) that change in time and image movement due to relative machine/periscope/camera motion that routinely exceeds 20 pixels. To compensate for the image movement, the overall tile pattern is used as a landmark to numerically stabilize the image, requiring the wide field-of-view seen in Fig. 1. Nevertheless, the camera/periscope system resolves ~ 1 mm scale features on the ramped-tile surfaces. In-situ cross calibrations of the IR emission with the embedded thermocouples are performed after each shot while the tiles are still hot, correcting for changes in emissivity due to surface film evolution and for degradations in periscope transmission [2].

An array of 10 Langmuir probes is embedded in divertor tiles at a toroidal location that is 90 degrees away from the ramped tiles with similar poloidal spacing as the thermal sensors. These record profiles of plasma density and electron temperature at ~ 5 ms intervals, yielding estimates of parallel heat fluxes via standard sheath models. Langmuir probe and calorimeter data provide valuable cross-checks on the IR-inferred heat flux profiles and allow basic tests of plasma-sheath heat transmission [3].

A 2-D finite-element heat transfer model (QFLUX_2D) is used to infer surface heat fluxes from surface temperature measurements. QFLUX_2D employs a fully implicit time-integration scheme with an accurate description of the tile/plate geometry, including tile gaps (see Fig. 2) and temperature-dependent materials properties. Surface films can dramatically alter the relationship between surface temperature and heat flux, and if not properly considered, can lead to erroneous negative heat fluxes [4]. We employ a novel Fourier analysis method to estimate the thermal resistance of films: (1) computing the complex thermal impedance of a bare surface using measured temperatures and modeled heat fluxes and (2) adding to this a minimal amount of surface thermal resistance to eliminate negative

heat fluxes. The bottom panel of Fig. 2 shows the output of this computation, expressing the surface thermal resistance in terms of its equivalent thickness of a pure boron film.

3. EDA H-mode discharges

Armed with these new diagnostics, we have begun an experimental program to investigate heat flux footprints and their corresponding mid-plane mapped boundary layer profiles over a wide range of parameters. Here we restrict our attention to initial results from EDA H-mode discharges with varying plasma currents ($I_p = 0.5, 0.8, 0.9, 1.0$ MA), toroidal magnetic fields ($B_T = 4.5, 5.4, 6.2$ tesla) and ICRF input powers ($P_{ICRF} = 0$ to 4.5 MW) in a standard lower-single null configuration ($\kappa \sim 1.6$, $\delta_L \sim 0.48$, $\delta_U \sim 0.32$). Due to damaged tungsten tiles on the outer divertor (3rd tile row from the bottom in Fig. 2), the strike point location was restricted to reside on or above the 4th tile row for all the discharges reported here.

EDA H-modes are steady-state discharges in which the pedestal is regulated by a continuous ‘quasi-coherent’ edge mode, rather than by a regular procession of ELMs [5]. Figure 3 shows a representative 0.9 MA, 5.4 tesla EDA H-mode discharge, with 4 MW of ICRF power (80 MHz, second-harmonic, hydrogen-minority). Radiated power from the confined plasma (P_{RAD}) is deduced from a resistive bolometer system [6], providing an estimate of the power into the scrape-off layer (P_{SOL}). Power onto the outer divertor (P_{ODIV}) is computed from the IR-inferred divertor heat flux profiles.

Heat flux footprints are found to exhibit a two zone structure: a narrow ‘power channel’ near the separatrix of approximately ~ 2 mm wide (characterized by its full-width at half-maximum, FWHM), and a ‘tail’ that extends into the far SOL region. It should be noted that the exact location of the separatrix relative to the narrow heat flux channel is uncertain, with shot-to-shot variation on the order of ~ 1 mm and systematic offsets on the same order.

Langmuir probe data verify that the ‘tail’ feature in the heat-flux profile is real and not some artifact of the IR-inferred heat flux profile. Langmuir probes are not able to spatially resolve the narrow feature, however; parallel heat fluxes in this region ($> \sim 300 \text{ MW m}^{-2}$) often exceed the range in which tungsten probes can operate without melt damage.

Following the definition by Loarte [7], the integral heat flux width (integral λ_q), is found to be $\sim 3 \text{ mm}$ for this discharge. Although the ‘tail’ feature affects this definition, the integration is nonetheless performed over the full profile, from -5 to 15 mm mapped to the outer midplane. Integral λ_q values are found to differ substantially from the scalings of Kirnev *et al.* [8], which project to 0.55 mm (conduction-limited case, as observed) and 1.0 mm (convection-limited case) for the discharge in Fig. 3. However, the authors appropriately warn: “The main problem in the extrapolation ... is the scaling of λ_q with the major radius, which cannot be inferred from experiments and simulations on JET alone.” This uncertainty in major radius scaling is a primary impetus for undertaking the experiments reported here. Empirical scaling laws compiled by Loarte *et al.* [7] align with the C-Mod observations, projecting to 5.2 mm (H-1, based on *PODIV*) and 3.4 mm (H-2, based on *PSOL*). It is important to point out that if the Loarte scaling holds true for ITER, integral λ_q values would be $\sim 20 \text{ mm}$ [7] rather than $\sim 4 \text{ mm}$ [8] – another strong motivation for the present work.

4. Effect of magnetic connection length

In addition to the experiments described above, a small set of discharges ($I_p = 0.5, 1.0 \text{ MA}$, $B_T = 5.4 \text{ tesla}$) were run with the x-point balance changed dynamically; the magnetic equilibrium was programmed to start in lower single-null and approach a double-null configuration. The goal of these experiments was to document changes in the divertor heat flux footprint as the magnetic connection length changed (a factor of ~ 2 longer for single-null

versus double-null). The result from these initial experiments can be simply stated: the shape of the heat flux profile remained unchanged as the location of the secondary separatrix swept across the outer divertor face.

This result may seem puzzling at first but is consistent with previous C-Mod observations of scrape-off layer (SOL) profiles in response to magnetic topology changes [9]: in changing from single to double-null, the electron pressure profiles in the low-field side SOL remained similar. Taken together, these observations suggest that the heat flux profile on the outer divertor is set largely by transport and associated ‘critical gradients’ on the low-field side; whether the field line connects a long way around to the inner divertor (single-null) or a short way to the upper divertor (double null) is apparently not of primary importance.

5. Connections to H-mode pedestal and confinement

A number of important heat flux footprint observations are clearly illustrated in the time sequence of a 1.0 MA, 5.4 tesla EDA H-mode discharge shown in Fig. 4. This plasma exhibited two separate EDA phases (EDA 1, EDA 2), with a clear quasi-coherent mode present in both. During EDA 1, the ramp-up in ICRF power combined with increasing P_{RAD} resulted in a 50% modulation in the peak heat flux arriving at the outer divertor. Yet, the shape of the heat flux profile is found to be invariant during this phase. Thus, the level of power into the scrape-off layer does not explicitly influence the width of the heat flux footprint. Moreover, integral λ_q steps up from 4 mm (EDA 1) to 5 mm (EDA 2) with essentially no change in external control parameters. These observations clearly confound efforts to characterize λ_q as a simple power-law function of global engineering quantities.

As shown in panel (c) of Fig. 4, electron pressures at the top of the pedestal were significantly reduced in the transition from EDA 1 to EDA 2. Associated with this is a flattened pressure profile in the SOL. This behavior has been noted before in C-Mod – as

confinement improves, SOL pressure gradient scale lengths become shorter [10]. ASDEX-Upgrade examined similar relationships, producing an explicit power-law scaling of heat flux widths in terms of H-mode confinement factor [7]. Thus, one must look to the physics of the edge transport barrier and pedestal as controlling the width of the power channel in the SOL.

Finally, heat flux widths from the full set of EDA H-mode discharges are compiled in Fig. 5. Heat flux widths are found to systematically decrease with increasing plasma thermal energy, consistent with the above pedestal observations (note locations of EDA 1 and EDA 2 data points). Since plasma thermal energy increases roughly with plasma current squared, heat flux widths have a tendency to decrease with increasing plasma current. While the variation of toroidal field in the present data set is modest (factor of 1.5), no explicit dependence on this parameter is evident – an observation that also makes contact with the pedestal, where pressure gradients are insensitive to toroidal magnetic field strength [11].

Acknowledgments

This work is supported by U.S. D.o.E. Coop. Agreement DE-FC02-99ER54512.

References

- [1] R.J. Maqueda, *et al.*, *Rev. Sci. Instrum.* 70 (1999) 734.
- [2] J.L. Terry, *et al.*, submitted to RSI (2010).
- [3] D. Brunner, *et al.*, these proceedings (2010).
- [4] A. Hermann, "Limitations for divertor heat flux calculations of fast events in tokamaks," presented at the 28th EPS Conference on Controlled Fusion and Plasma Physics, Madeira, Portugal, 2001.
- [5] M. Greenwald, *et al.*, *Phys. Plasmas* 6 (1999) 1943.
- [6] M.L. Reinke and I. Hutchinson, *Rev. Sci. Instrum.* 79 (2008) 10F306.
- [7] A. Loarte, *et al.*, *J. Nucl. Mater.* 266-269 (1999) 587.
- [8] G. Kirnev, *et al.*, *Plasma Phys. Control. Fusion* 49 (2007) 689.
- [9] B. LaBombard, *et al.*, *Nucl. Fusion* 44 (2004) 1047.
- [10] B. LaBombard, *et al.*, in *Plasma Physics and Controlled Fusion Research 1996* (Proc. 16th Int. Conf. Montreal, 1996), IAEA, Vienna (1997) Vol. 1, 825.
- [11] J.W. Hughes, *et al.*, *Nucl. Fusion* 47 (2007) 1057.

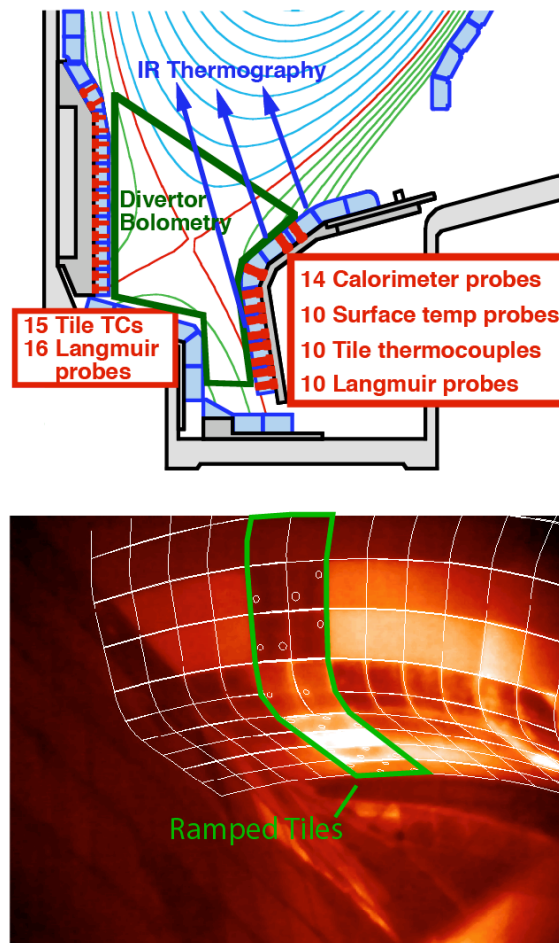


Fig. 1. Divertor heat flux diagnostics installed during the 2009 maintenance period. An array of calorimeter plus surface and tile temperature sensors is embedded into two vertical columns of ‘ramped tiles’ on a sector of the outer divertor (poloidal cross-section shown in top panel). Langmuir probes (indicated in red) are located in a different sector, displaced 90 degrees toroidally. IR camera/periscope system views a portion of the outer divertor and ramped tiles at an oblique angle (bottom panel). A virtual 3-D model of C-Mod’s first-wall tiles and periscope location is used generate an artificial image, yielding a reference tile grid for image alignment (overlaid).

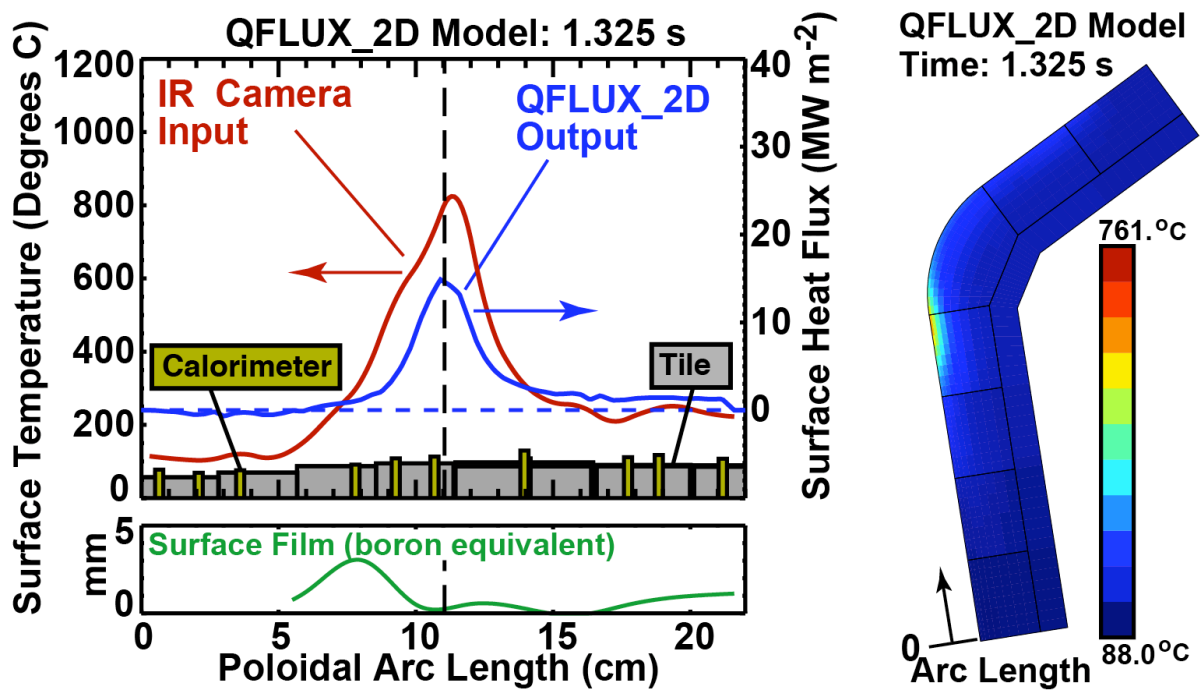


Fig. 2. A 2-D thermal transport model (QFLUX_2D) is used to infer surface heat fluxes from surface temperature measurements. Corrections are applied to account for the presence of surface films, which effectively add a thermal resistance layer. Tile and calorimeter temperature measurements are also shown (color bars). These are used to calibrate the IR camera system long after a shot when temperatures are equilibrated.

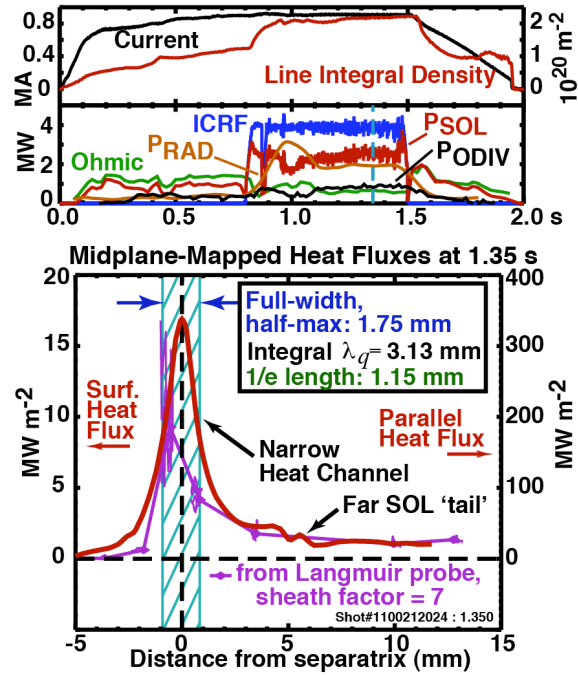


Fig. 3. Representative time traces (top panels) and a corresponding divertor heat flux footprint from a steady EDA H-mode discharge. Heat flux profiles from IR camera (red line, bottom panel) and Langmuir probe array (purple line) are shown, mapped to the outer midplane.

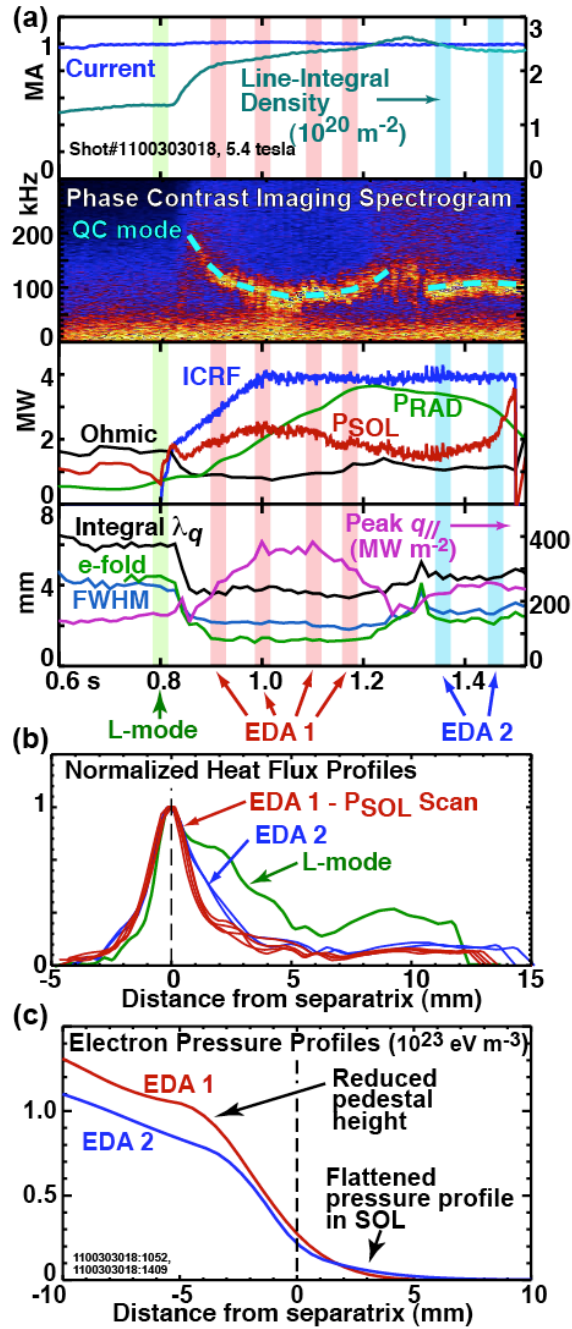


Fig. 4. H-mode discharge with two different time-evolving EDA phases (a). PSOL varies significantly during the first EDA phase (EDA 1). Yet, normalized heat flux profile shapes are virtually identical, despite the 50% modulation in peak parallel heat fluxes (b). In contrast, the second EDA phase (EDA 2) exhibits a wider heat flux footprint at comparable PSOL values. Pedestal electron pressure profiles are correspondingly different, with the ‘reduced confinement pedestal’ of EDA 2 displaying a flatter pressure profile in the SOL (c).

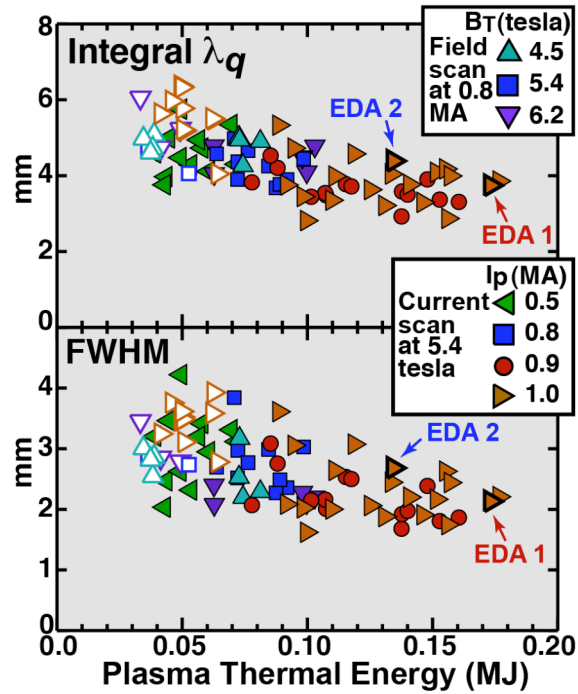


Fig. 5. Integral heat flux footprint widths are well correlated with plasma thermal energy (top panel). Data from all conditions studied thus far follow a similar scaling, even accommodating L-mode discharges (open symbols). Full-width, half-maximum values show a similar trend with more scatter (bottom panel). Because of these trends, heat flux widths in H-mode discharges tend to decrease with increasing plasma current. No explicit dependence on toroidal magnetic field strength is evident.